



# Interannual correlations between sea surface temperature and concentration of chlorophyll pigment off Punta Eugenia, Baja California, during different remote forcing conditions

H. Herrera-Cervantes<sup>1</sup>, S. E. Lluch-Cota<sup>2</sup>, D. B. Lluch-Cota<sup>2</sup>, and G. Gutiérrez-de-Velasco<sup>3</sup>

<sup>1</sup>Unidad La Paz, Centro de Investigación Científica y de Educación Superior de Ensenada (CICESE), La Paz, Baja California Sur 23050, México

<sup>2</sup>Centro de Investigaciones Biológicas del Noroeste (CIBNOR), Instituto Politécnico Nacional 195, La Paz, Baja California Sur 23096, México

<sup>3</sup>Departamento de Física, Universidad de Guadalajara, México

Correspondence to: H. Herrera-Cervantes (hherrera@cicese.mx)

Received: 26 April 2013 – Published in Ocean Sci. Discuss.: 29 May 2013

Revised: 7 March 2014 – Accepted: 24 March 2014 – Published: 14 May 2014

**Abstract.** Interannual correlation between satellite-derived sea surface temperature (SST) and surface chlorophyll *a* (Chl *a*) are examined in the coastal upwelling zone off Punta Eugenia on the west coast of the Baja California Peninsula, an area that has been identified as having intense biological productivity and oceanographic transition between midlatitude and tropical ocean conditions. We used empirical orthogonal functions (EOF) analysis separately and jointly on the two fields from 1997 through 2007, a time period dominated by different remote forcing: ENSO (El Niño–Southern Oscillation) conditions (weak, moderate and strong) and the largest intrusion of subarctic water reported in the last 50 years. Coastal upwelling index anomalies (CUI) and the multivariate ENSO index (MEI) were used to identify the influence of local (wind stress) and remote (ENSO) forcing over the interannual variability of both variables. The spatial pattern of the individual EOF<sub>1</sub> analysis showed the greater variability of SST and Chl *a* offshore, their corresponding amplitude time series presented the highest peaks during the strong 1997–2000 El Niño–La Niña cycles and during the 2002–2004 period associated to the intrusion of subarctic water. The MEI is well correlated with the individual SST principal component ( $R \approx 0.67$ ,  $P < 0.05$ ) and poorly with the individual Chl *a* principal component ( $R = -0.13$ ). The joint EOF<sub>1</sub> and the SST–Chl *a* correlation patterns show the area where both variables covary tightly; a band near the coast where the largest correlations occurred ( $|R| > 0.4$ ) mainly regulated

by ENSO cycles. This was spatially revealed when we calculated the homogeneous correlations for the 1997–1999 El Niño–La Niña period and during the 2002–2004 period, the intrusion of subarctic water period. Both, SST and Chl *a* showed higher coupling and two distinct physical–biological responses: on average ENSO influence was observed clearly along the coast in SST, while the subarctic water influence, observed offshore and in Bahía Vizcaíno, mostly in Chl *a*. We found coastal chlorophyll blooms off Punta Eugenia during the 2002–2003 period, an enrichment pattern similar to that observed off the coast of Oregon. These chlorophyll blooms are likely linked to high wind stress anomalies during 2002, mainly at high latitudes. This observation may provide an explanation of why Punta Eugenia is one of the most important biological action centers on the Pacific coast.

## 1 Introduction

Continuous oceanographic observations carried out on the west coast of Baja California by the CalCOFI (California Cooperative Oceanic Fisheries Investigations) and IMECOCAL (Mexican Research of the California Current) programs have helped define the region of Punta Eugenia (Fig. 1) as an oceanographic transitional zone (Durazo and Baumgartner, 2002), characterized by the interaction of subarctic and tropical waters (Almazán-Becerril et al., 2012) as a result of

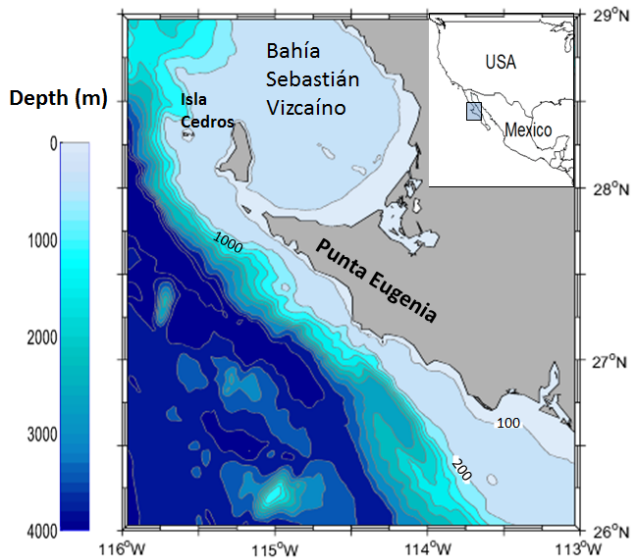


Fig. 1. Location and bathymetry characteristics of the study area.

the convergence of the southern part of the California Current (CC) and the North Equatorial Current (NEC). Its shelf is about 50–90 km wide, including Bahía Vizcaíno, this becomes narrow and almost disappears off Punta Eugenia (González-Rodríguez et al., 2012). The area is also influenced by warm and dense water originating in the Gulf of California (Parés-Sierra et al., 1997), creating a complex mixing zone between coastal and oceanic flows and intense mesoscale variability characterized by a complex pattern of filaments, meanders, and semipermanent eddy structures (Gallaudet and Simpson, 1994). These structures carry nutrient-rich coastal waters to deep areas, causing important seasonal variability and interannual and long-term changes in the mean field of variables as SST and Chl *a* (Espinosa-Carreón et al., 2004).

Seasonal wind forcing over the Punta Eugenia area is controlled regionally by the position and intensity of the North Pacific high pressure and the California semipermanent low thermal (Parés-Sierra et al., 1997). This wind pattern generates an intense coastal upwelling process that, together with the local contribution of the coastal lagoons (Guerrero Negro, Ojo de Liebre, and San Ignacio), produces one of the most important biological action centers (BAC) of the western coast of North America, which is characterized by above-average pigment concentrations (Lluch-Belda et al., 2000). The coastal ecosystem of this region is a natural refuge and a feeding and breeding area for many ecological and commercially important species (gray whale, sea turtles, spiny lobster, abalone, and clams). Maintenance of this ecosystem is based on three factors: rich coastal waters associated with an intense upwelling regime, successful implementation of cooperatives to safeguard existing resources, and relative isolation. These factors help support the fishery

and natural resources in this area, which includes red lobster (value of USD 65 million annually; Vega et al., 2010; SAGARPA, 2011), abalone (value of USD 26 million annually; SAGARPA, 2001), and extraction of salt by solar evaporation (7000 t annually; SEMARNAT, 1997) contributing to the economy of the entire peninsula.

Oceanographic features off the west coast of the Baja California Peninsula are dramatically affected by global-scale ENSO (El Niño–Southern Oscillation) and interdecadal variability. El Niño events have a negative effect on fisheries: an increase in SST, sea level height, change in composition of the zooplankton community, and microbial pollution (Strub and James, 2002; Lavaniegos et al., 2002; Hereu et al., 2003; Boehm et al., 2004). Larval reproduction, embryonic development and changes in abundance of spiny lobster (*Panulirus interruptus*) are heavily impacted by El Niño–La Niña events (Vega et al., 2010) because the onset and duration of breeding is accelerated or delayed (Vega, 2003), which dramatically reduces the captures in this region. Carreón-Palau et al. (2003) and Muciño-Días et al. (2004), describe serious decline of abalone because survival, growth, and larval recruitment are heavily dependent on cooler environmental conditions. These relationships between biological and environmental factors demonstrate strong physical–biological coupling in this region.

Climate effects on SST and Chl *a* in this coastal environment are well documented here due to more than a decade of satellite measurements (1997–2007). This period includes different ENSO conditions (weak, moderate and strong) well illustrated by the 1999–2004 period of increasing MEI (multivariate ENSO index; Behrenfeld et al., 2006), beginning with strong El Niño/La Niña cycles between 1997 and 1999, followed by a weak El Niño between 2002 and 2004, and finally a moderate El Niño during the 2006–2007 period. Additionally, during the 2002–2004 period the California Current System (CCS), remained in the cold phase (Goericke et al., 2005), a state it has maintained since the 1999 La Niña phase with the presence of the largest intrusion of subarctic water reported in the last 50 years, which is characterized as a cold and fresh anomaly in the upper halocline (Huyer, 2003).

In this study, we explored the interannual covariance between SST and Chl *a* off Punta Eugenia, an adequate area as a reproductive habitat due to high levels of biological production and its responses to two different large-scale processes; the ENSO cycles and the intrusion of subarctic water. Individual and joint empirical orthogonal functions (EOF) analyses were used to extract the principal modes of interannual variability and correlation patterns to analyze statistically the temporal and spatial coupled modes of variability between SST and Chl *a* and their response to warming and cooling climate processes. Additionally, we examine time series of coastal anomalies of SST, Chl *a* and wind stress to observe the propagation of the ENSO signals and subarctic water intrusion during two different time periods: 1997–2007 and 2002–2004.

## 2 Data and methods

The data used in this analysis are monthly composites of SST and Chl *a* satellite images covering the period from September 1997 through to December 2007 for an area 26–29° N and 113–116° W, centered at Punta Eugenia (see Fig. 1). These data are derived from an advanced very high resolution radiometer (AVHRR-Pathfinder) sensor for SST and sea-viewing wide field-of-view sensor (SeaWiFS) for Chl *a*, available at their respective internet addresses (<http://podaac.jpl.nasa.gov/> and <http://oceancolor.gsfc.nasa.gov/SeaWiFS>). O'Really et al. (2000), Kahru and Mitchell (2001) as well as Mitchell (2004) have shown that the CalCOFI and IMECO-CAL regions are ideal locations to evaluate the accuracy, precision and suitability of ocean color chlorophyll algorithms. Comparison of in situ and SeaWiFS Chl *a* estimates using these algorithms tends to produce a higher coefficient of determination ( $r^2 \approx 0.9$ ) and a smaller root-mean-square error (RMSE  $\approx 0.2$ ); nevertheless, Kahru and Mitchell (2001) and Mitchell (2004) found that discrepancies between satellite-derived Chl *a* data and in situ values at near-shore CalCOFI stations may be caused by small-scale spatial variability.

After rotating and orienting the images along the coast, the 9 km  $\times$  9 km Chl *a* initial grid was interpolated using a MATLAB function into a 4 km  $\times$  4 km pixel array to produce the same spatial resolution used in the SST. These processes resulted in matrices of monthly composite images of SST ( $x, t$ ) or Chl *a* ( $x, t$ ) values where  $x$  stands for the cells of each image and  $t$  stands for each month between September 1997 and December 2007. To remove the annual and semiannual signals, we fitted the monthly time series of each pixel to the periodic function as follows:

$$F(t) = A_0 + A_1 \cos(w_1 t - \varphi_1) + A_2 \cos(w_2 t - \varphi_2), \quad (1)$$

where  $A_0$  is the annual mean,  $A_1$ ,  $w_1$ , and  $\varphi_1$  are the amplitude, frequency, and phase of the annual signal and  $A_2$ ,  $w_2$ , and  $\varphi_2$  are the equivalent of the semiannual signal. Next, we obtained the matrices of SST and Chl *a* anomalies (interannual variability), subtracting from each time series of each cell its corresponding fitted periodic function (Eq. 1) as

$$\mathbf{A}(x, t) = \mathbf{M}(x, t) - \mathbf{F}(x, t). \quad (2)$$

Each non-seasonal anomalies matrix was transformed into normalized anomalies  $\text{NA}(x, t)$  by dividing  $A(x, t)$  series of each pixel by its standard deviation. The resulting  $\text{NA}(x, t)$  matrices of both variables were used in the individual EOF analysis to identify the dominant modes of SST and Chl *a* interannual variability and its evolution over time (principal components). Joint EOF analysis is calculated from the covariance matrix constructed from both variables to highlight how they covary with each other (Wilson and Adamec, 2001). Additionally we calculated homogeneous correlations (Bretherton et al., 1992), the correlation at each point between the SST and Chl *a* data and its corresponding EOF<sub>1</sub>

temporal components for two subsets of the time series, between September 1997 and December 1999 and between January 2002 and December 2003, these time periods are chosen using the temporal evolution of the individual SST and Chl *a* principal component alongside the MEI. The integral timescale of these homogeneous correlations and the effective number of degrees of freedom would lead to an expected artificial correlation (Davis, 1976; Sciremammano, 1979; Chelton, 1982; and Tremberth, 1983), however its spatial distribution could delineate the regions that contribute the most to the mode 1 during different time periods (Wilson and Adamec, 2001).

Indices of the intensity of large-scale, wind-induced coastal upwelling (CUI) are generated by the NOAA/NMFS (National Marine Fisheries Service) Pacific Fisheries Environmental Laboratory (PFEL) at 15 standard locations along the west coast of North America (Schwing and Mendelssohn, 1996; <http://www.pfeg.noaa.gov/>). We used the CUI centered on 27° N, 116° W, as representative of the Punta Eugenia coastal region, filtering out the seasonal cycle by subtracting the corresponding climatological monthly average (CUI interannual anomalies time series). ENSO activity was represented by the MEI, a measure of the variability of the Pacific (Wolter and Timlin, 1993; Behrenfeld et al., 2006). We note that, though these indices summarize variability over different regions and the correlation between them are not large, wind data used to build monthly CUI anomalies in this region are strongly affected by ENSO events and are not completely independent (Storch and Zwiers, 1999). CUI and MEI values were normalized by dividing the time series by its standard deviation prior to calculating correlation values to make a more meaningful indicator of the true degree of linear relation with local SST and Chl *a* changes (Sciremammano, 1979).

Finally, to observe the evolution of the intrusion of subarctic water within the  $\sim 50$  km closest to the coast of North America (22–45° N) including the coast of the study area and its relationship with the Chl *a* and wind forcing, we built time plots (Hovmöller diagrams) based on time series of coastal Chl *a* and wind stress anomalies data between January 2002 and December 2003. For this last analysis we used Chl *a* weekly 18 km  $\times$  18 km pixel array composites filtering out the seasonal cycle subtracting the Chl *a* weekly climatology provided by the SeaWiFS (Sea-viewing Wide Field-of-view Sensor) project. The wind stress anomalies ( $\text{N m}^{-2}$ ) was calculated in the same way that the matrices of SST and Chl *a* used in the individual EOF analysis, using monthly mean ocean surface wind in a 0.25°  $\times$  0.25° pixel array composite provided by the Cross-Calibrated Multi-Platform (CCMP) project website at <http://podaac.jpl.nasa.gov/dataset/> and re-binned into 18 km  $\times$  18 km to have the same spatial resolution used in Chl *a* weekly composites.

### 3 Results

To determine the regions off Punta Eugenia where SST and Chl *a* have the largest seasonal fluctuations, the standard deviation (SD) variability is calculated for each monthly time series of the satellite-derived  $SST(x, \tilde{t})$  and  $Chl\ a(x, \tilde{t})$  observations (Fig. 2). Both patterns had large gradients along the coast and the largest seasonal fluctuations in SST ( $>3\ ^\circ\text{C}$ ) and Chl *a* ( $>1\ \text{mg}\ \text{m}^{-3}$ ) near to the coast, mainly south of Punta Eugenia and north of Isla de Cedros. The deep zone presented the lowest values, this included Bahía Vizcaíno where the barotropic circulation associated to a semipermanent anticyclonic gyre (Palacios et al., 1996) could mask the amount of biological productivity. This pattern is consistent with near shore eutrophic conditions and/or oligotrophic conditions farther offshore (Kahru and Mitchell, 2000). The bottom panels represent the time plot of SST, Chl *a*, and CUI (space-averaged  $SST(x, \tilde{t})$  and  $Chl\ a(x, \tilde{t})$  and CUI monthly time series), all dominated by strong annual cycle (right panel), although large interannual changes were still evident. High peaks of Chl *a* and CUI (spring–summer) seem to show a trend to increasing annual maxima mostly (higher maxima) during the 2002–2003 period, Kahru and Mitchel (2001), using monthly composites of a four ocean color sensors-derived Chl *a* data set, showed a similar behavior in coastal areas off Baja California. The three parameters reveal coincidences between them.

Figure 3 shows the interannual variability of SST and Chl *a* off Punta Eugenia conformed by a single dominant mode. The spatial patterns of the individual EOF analyses (surface plot of the EOF<sub>1</sub> loadings; panels a, b), account for 78 and 45 % of the total variance for SST and Chl *a* (with the sign-reversed) respectively. Both variability patterns were not spatially homogeneous, strong gradients and high loadings were observed in a broad band along the coast but tended to be low near to the coast as distinct from the standard deviation maps (Fig. 2). The amplitude time series (time plot of the EOF<sub>1</sub> score; lower panel c) showed that the SST interannual variability was forced by ENSO-related events (e.g., the signals of the 1997–1998 El Niño, 1999–2000 La Niña and 2006–2007 El Niño) showing a major correlation with the MEI while the principal components of Chl *a* presented the higher amplitude peaks during the 2002–2004 period. The correlations values between the principal components of individual EOF analyses (SST and Chl *a*) and the normalized time series of MEI and CUI anomalies are presented in Table 1. The MEI is well correlated with the individual SST principal component ( $R = 0.67$ ,  $P < 0.05$ ) and poorly with the individual Chl *a* principal component ( $R = -0.13$ ), while the CUI correlation with these same principal components is low in both cases ( $R = -0.13$  and  $R = 0.20$ ), suggesting that the SST interannual variability was forced principally by ENSO conditions observed during the entire period (weak, moderate, and strong) while the main forcing in the Chl *a* interannual variability could be associated to the

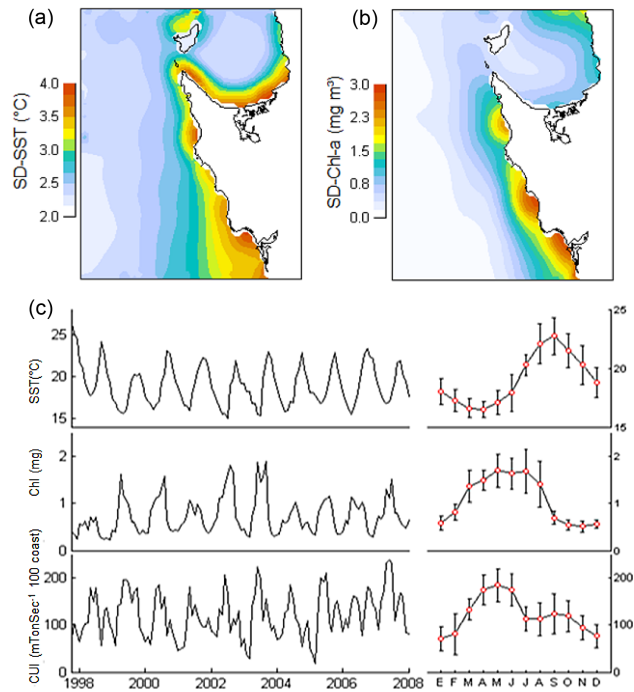


**Fig. 2.** Surface plots of standard deviation variability (time averaged) and monthly time series (spatial averaged) of the satellite-derived SST and chlorophyll *a* compared with the monthly CUI time series calculated from the Pacific Fisheries Environmental Group (PFEG) website (<http://www.pfeg.noaa.gov/>) for the Punta Eugenia region ( $27^\circ\ \text{N}$ ,  $116^\circ\ \text{W}$ ). The curves on the right side correspond to the average seasonal cycle for each variable. Observed averages (red circles) and vertical bars indicate standard deviation.

intrusion of subarctic water represented by the high peaks in the amplitude time series of the Chl *a* during the 2002–2004 period.

Figure 4 shows the spatial pattern of the first mode of the joint EOF<sub>1</sub> analysis for SST and Chl *a* (panels a, b), accounting for 80 % of the total variance. The amplitude time series corresponding to the joint EOF<sub>1</sub> is not shown since it is virtually identical to those of individual SST components shown in Fig. 3c, having a correlation of 0.98 (see Table 1). The joint spatial modes (SST and Chl *a*), differ to those of the individual EOF<sub>1</sub> (Fig. 3a, b). The primary difference is that the coastal and northern region dominates more in the joint EOF, mostly in the chlorophyll mode (Fig. 4b) where the northern area of Punta Eugenia and Bahía Vizcaíno shows the largest spatial loadings. In the joint mode, low variability corresponds to the depth and southern region as a continuous feature. The spatial distribution of the correlation coefficient between monthly anomalies of SST and Chl *a* (Fig. 4c), present the area where both parameters strongly co-vary. This area (a band parallel to the coast) is enclosed with the highest correlations values ( $|R| > 0.25$ ) and is similar with the area where the joint EOF<sub>1</sub> scores of the SST (Fig. 4a) are  $> 2.0$ . Correlations above  $R_{\text{crit}}$  ( $P < 0.05$ ) = 0.211, i.e., the strongest

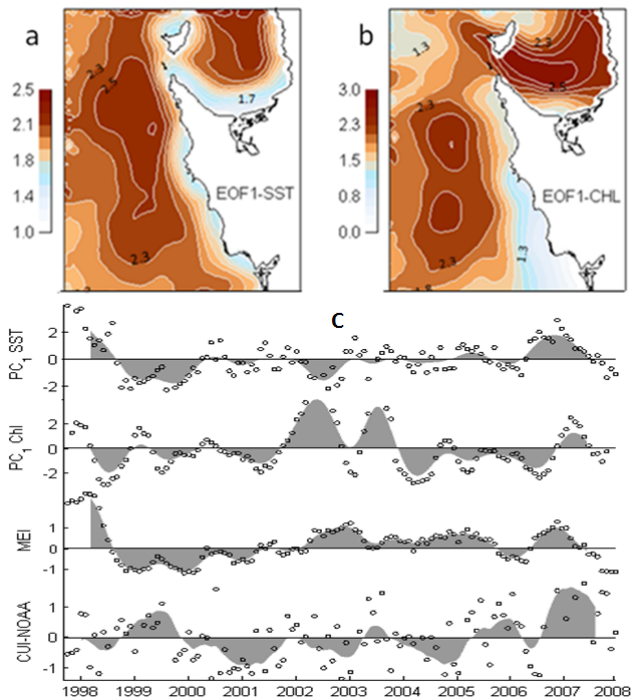


**Fig. 3.** Spatial patterns for mode 1 of the individual EOF analyses. (a) SST, (b) chlorophyll *a*. This mode accounts for 78 and 45 % of the total variance for SST and chlorophyll *a* (with the sign reversed), respectively. (c) Time-series data indicate the temporal evolution of the EOF1 alongside the MEI and monthly CUI anomalies (dots), all smoothed by a five-term running mean (shaded area).

negative correlation in the blue areas, are statistically significant ( $P < 0.05$ ). Correlations that are not statistically significant at the 95 % level are shaded light blue.

Figure 5 shows contours of mean homogeneous correlation calculated for two subsets of the time series, between September 1997 and December 1999 and between January 2002 and December 2003, in both SST and Chl *a* respectively. Correlations between the shorter SST and Chl *a* time series of the data and its corresponding temporal components are given in Table 2 along with  $N$  the number of values of each subset,  $\tau$  the integral timescale,  $N_{\text{eff}}$  the effective degree of freedom, the Student  $t$  value and  $P_{\text{val}}$  the statistical significance. The integral timescale of these homogeneous correlations for the ENSO cycle ( $\tau_{\text{SST}} = 3.7$  and  $\tau_{\text{Chl } a} = 2.0$ ) and for the subarctic period ( $\tau_{\text{SST}} = 1.5$ ,  $\tau_{\text{Chl } a} = 1.9$ ) could not be regarded as significant but can be used to assess what regions dominate during these periods. There are significant similarities between the homogeneous correlations distribution during the El Niño–La Niña period (solid and dotted contours in Fig. 5a); a narrow area confined along the coast dominates during this period, this distribution is virtually identical to the spatial correlation pattern showed in Fig. 4c (gray regions delineate areas with absolute correlations greater than 0.25), meaning that the physical–biological

**Table 1.** Correlation coefficients between principal components from different SST and chlorophyll *a* EOF<sub>1</sub> analyses (individual (ind.) and joint) and MEI and monthly CUI anomalies using the original time series ( $N = 124$ ).

|                           | EOF <sub>1</sub><br>ind. SST | EOF <sub>1</sub><br>ind. Chl | EOF <sub>1</sub><br>joint | MEI   | CUI |
|---------------------------|------------------------------|------------------------------|---------------------------|-------|-----|
| EOF <sub>1</sub> ind. SST | 1.0                          |                              |                           |       |     |
| EOF <sub>1</sub> ind. Chl | 0.21                         | 1.0                          |                           |       |     |
| EOF <sub>1</sub> joint    | 0.98                         | 0.97                         | 1.0                       |       |     |
| MEI                       | 0.67                         | −0.13                        | 0.63                      | 1.0   |     |
| CUI                       | −0.13                        | 0.20                         | 0.17                      | −0.13 | 1.0 |

coupling shown in the coastal region is driven by both increase and decrease of SST and chlorophyll during ENSO cycles. In contrast, during the period of subarctic water intrusion the highest mean homogeneous correlations distribution (solid contours in Fig. 5b) are located in the central basin along the coast and over Bahía Vizcaíno, a region where individual EOF patterns show the high variability mainly in the chlorophyll mode (dark gray regions delineate areas with absolute Chl *a* spatial loadings greater than 2.3). These results delineate the regions that contribute the most to the individual and coupled modes during different remote forcing periods, indicating that the individual variability pattern of both parameters could be driven more by the intrusion of subarctic water than by ENSO cycles.

Figure 6 shows the time series of (a) the MEI index (bars) and CUI anomalies (curves), both compared with the temporal evolution of (b) SST and (c) Chl *a* coastal anomalies signals plotted in two Hovmöller diagrams (i.e., time series of coastal pixels plotted as contours) from 26° N (at the bottom of the diagrams) to the north of Bahía Vizcaíno (at the top, the black line in the middle indicates the position of Punta Eugenia on the coast). Monthly CUI anomalies time series are partially impacted by the different ENSO cycles (weak, moderate and strong), in phase but negatively correlated with the MEI in most of the time period. Panel b shows that coastal anomalies of SST are associated with ENSO events mainly at the strong 1997–1998 El Niño event, where the maximum SST anomalies (from ~ 3 to −2 °C) in the south of Punta Eugenia are transmitted to Bahía Vizcaíno with a slight attenuation mainly during the 1998–2000 La Niña event whose influence abruptly finalizes prior to that shown by MEI. Previous to the weak 2002–2004 El Niño event, the SST anomalies showed a short warm period. A strong cold event was observed at the beginning of 2002, with high concentration of negative anomalies (~ −3 °C) observed mainly in Bahía Vizcaíno, which remained stationary along the entire coast through the end of 2005 with a slight attenuation after 2003 south of Punta Eugenia. The 2006–2007 El Niño event, caused the end of the previous cold event, SST anomalies of ~ 2 °C were observed mainly on the southern

**Table 2.** Correlations between  $N$  monthly SST and Chl  $a$  time series of the data and its corresponding principal components of individual EOF analyses for two subsets: ENSO period (September 1997–December 1999) and Subarctic period (January 2002 and December 2003) along with  $\tau$  the integral timescale,  $N_{\text{eff}}$  the effective degree of freedom, Student's  $t$  value and  $P_{\text{val}}$  the statistical significance. Correlation significance levels were obtained consulting classical statistical tables and using the methodology proposed by Davis (1976) and Trenberth (1983).

|                     |                         | $R$   | $N$ | $\tau$ | $N_{\text{eff}}$ | Student's<br>$t$ value | $P_{\text{val}}$       |
|---------------------|-------------------------|-------|-----|--------|------------------|------------------------|------------------------|
| ENSO<br>period      | SST vs. PC <sub>1</sub> | 0.99  | 28  | 3.7    | 7                | 96.0                   | $5.60 \times 10^{-10}$ |
|                     | CHL vs. PC <sub>1</sub> | -0.83 | 28  | 2.0    | 13               | 5.1                    | $2.50 \times 10^{-4}$  |
| Subarctic<br>period | SST vs. PC <sub>1</sub> | 0.99  | 24  | 1.5    | 15               | 48.0                   | $3.13 \times 10^{-16}$ |
|                     | CHL vs. PC <sub>1</sub> | -0.91 | 24  | 1.9    | 12               | 7.2                    | $2.48 \times 10^{-5}$  |

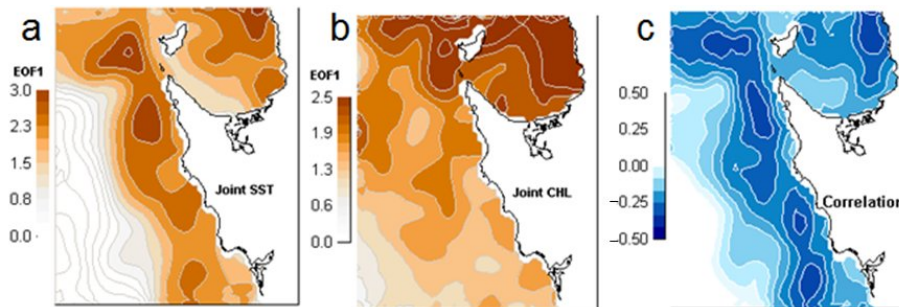


**Fig. 4.** Spatial patterns for mode 1 of the joint EOF analyses of (a) SST, (b) chlorophyll  $a$  (accounting for 80 % of the total variance) and (c) the correlation map between monthly anomalies of SST and chlorophyll  $a$ . The largest negative correlations ( $< -0.2$ , the blue areas) are seen along the coast and coincide with the high joint EOF<sub>1</sub> scores ( $> 2.0$ ) of SST (a). Absolute correlations above  $R_{\text{crit}}$  ( $P < 0.05$ ) = 0.211, (i.e., the strongest negative correlation) are significant at the 95 % confidence level.

coast of Punta Eugenia with a slight attenuation in Bahía Vizcaíno.

Panel c shows that coastal anomalies of Chl  $a$  are associated with ENSO events only at the beginning of the period; the strong 1997–1999 ENSO events where the Chl  $a$  anomalies showed high negative anomalies (from  $\sim -2$  to  $1.5 \text{ mg m}^{-3}$ ). Moderated concentrations occurred during the peaks of the 1998–2000 La Niña conditions, mainly south of Punta Eugenia with a strong attenuation when the signal are transmitted to Bahía Vizcaíno. During the weak 2002–2004 El Niño event, Chl  $a$  showed unusual behavior, higher concentrations ( $1.8\text{--}2.0 \text{ mg m}^{-3}$ ) occurred during this period along the entire coast. Positive anomalies remained stationary mainly in the coast of Bahía Vizcaíno through the end of 2006. The moderate 2006–2007 El Niño did not appear to have a noticeable effect on the coastal anomalies of Chl  $a$ , though it continued to have positive anomalies, maybe influenced by the positive phase showed by the CUI during the 2005–2007 period. These conditions (positives anomalies) were maintained until the end of the study period.

Figure 7 shows the relationship between the wind stress and Chl  $a$  anomalies during the period of subarctic water intrusion (January 2002–December 2003) in an area close to the coast of North America ( $22\text{--}45^\circ \text{ N}$ ). Latitude–time plots of (a) anomalies of monthly wind stress (magnitude and

direction;  $\text{N m}^{-2} \times 10^{-2}$ ) showed weak wind stress anomalies in early 2002 but increasing in intensity during spring–summer of 2002 (onshore direction). Anomalous wind stress along the northeastern Pacific coast may drive enhanced coastal upwelling and anomalous Ekman transport along the immediate coast (Taylor et al., 2008). Coastal Chl  $a$  anomalies (b) showed in detail that the southern coast, which includes from the study area (shaded in green) to the tip of the peninsula, presented high positive anomalies in Chl  $a$  ( $> 2.5 \text{ mg m}^{-3}$ ). It should be noted that the Chl  $a$  signals off Punta Eugenia, reach bloom conditions compared to that found north of  $42^\circ \text{ N}$  (off the Oregon coast), where the presence of the cold and fresh subarctic water masses in the CCS was first noticed (Kosro, 2003; Freeland et al., 2003; Goericke et al., 2005). High positive Chl  $a$  coastal anomalies, continued off Baja California during spring and summer 2003, without any significant delay or attenuation by the co-occurring 2002–2003 El Niño event (Bograd and Lynn, 2003; Durazo et al., 2005), while wind stress anomalies showed a pronounced decline.

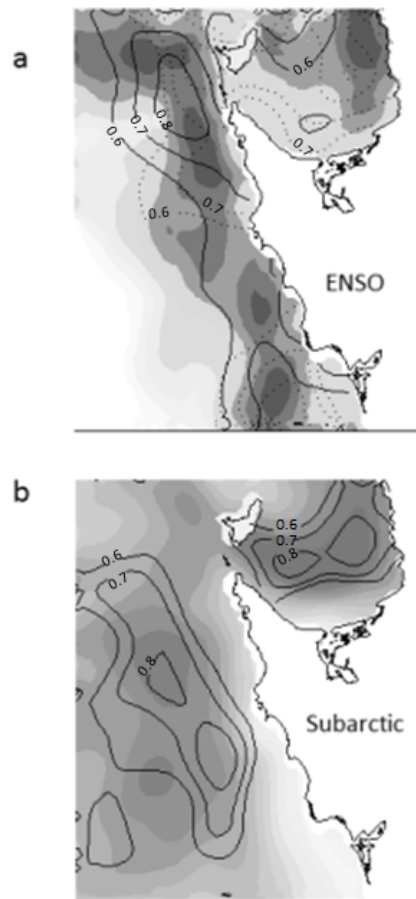


**Fig. 5.** Contours of mean homogeneous correlation between SST and Chl *a* for the El Niño and La Niña period (solid and dotted contours) overlaid on (a) the correlation map. Mean homogeneous correlation for the intrusion of subarctic water period (solid contours) overlaid on (b) mode 1 of the individual EOF analyses of chlorophyll *a*. The El Niño correlation is done using data from September 1997 through to December 1998; the La Niña correlation is done using data from September 1998 through to December 2000; and the subarctic water correlation is done using data from January 2002 through to December 2003. The contour interval is 0.1 and the minimum contour shown is 0.6.

#### 4 Discussion

In this study, we used EOF analysis both separately and jointly over satellite-derived SST and Chl *a* anomaly data off Punta Eugenia, a region with high levels of biological productivity that is associated with wind-driven upwelling processes (González-Rodríguez et al., 2012; Lluch-Belda et al., 2000), which has allowed us a wide-ranging view of the biophysical coupling during ENSO events and the largest intrusion of subarctic water reported in the last 50 years (Huyer, 2003; Venrick et al., 2003). Moreover, by relating each SST and Chl *a* series within  $\sim 30$  km of the coast of Punta Eugenia to two independent variables, MEI and CUI, and by following the coastal signal of the Chl *a* related to the intrusion

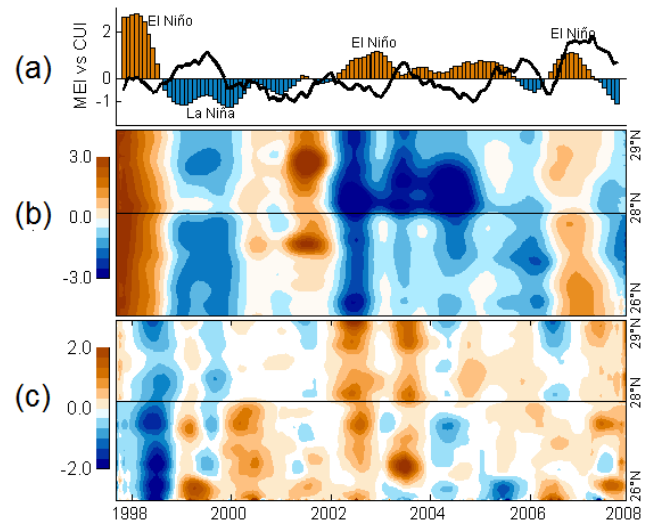


**Fig. 6.** Temporal evolution of (a) the MEI and monthly CUI anomalies. El Niño (La Niña) episodes are indicated by orange (blue) bars respectively as reported by the Climate Prediction Center of the National Center of Environmental Prediction at the National Oceanic and Atmospheric Administration (CPC-NCEP-NOAA). Hovmöller diagram of monthly averaged coastal SST anomalies (b) and chlorophyll *a* anomalies (c), from September 1997 to December 2007, covering approximately 300 km of coastline, from 26° (bottom graph) to 29° N (upper graph). Solid line indicates the position of Punta Eugenia on the coast (28° N).

of subarctic water from 45 to 22° N; to our knowledge, this is the first time that physical–biological covariability driven by remote forcing (tropical and subarctic origin) off Punta Eugenia has been examined at this level of detail.

The spatial patterns of individual EOF<sub>1</sub> (Fig. 3a, b) showed that the interannual variability of SST and Chl *a* are not homogeneous and have a strong gradient along the coast. Although both patterns are similar, its principal components are markedly different ( $R \approx 0.21$ ; see Table 1). The statistical relationship between the principal components of the SST mode and the MEI showed similar trends and were well correlated ( $R = 0.67$ ,  $P < 0.05$ ), except with the CUI anomalies time series (see Table 1). This may indicate that they were forced at the beginning of the time period by ENSO-related events but during the 2002–2004 period both SST and Chl *a* were forced by the large intrusion of subarctic water reported in the last 50 years (Venrick et al., 2003; Bograd and Lynn, 2003; and Durazo et al., 2005; Goericke et al., 2005), which masked the presence of the El Niño event in this period. Chl *a* reached the highest peak of variability during this period (Fig. 3c), suggesting that Chl *a*, unlike SST, was mostly affected by the intrusion of subarctic water. In this case the individual variability pattern of Chl *a* could be defined as the subarctic water mode. For the 1999–2006 period, a period with a sustained increase in MEI values (Berenfeld et al., 2006), the time series show a similar behavior. At the regional scale both warming and cooling

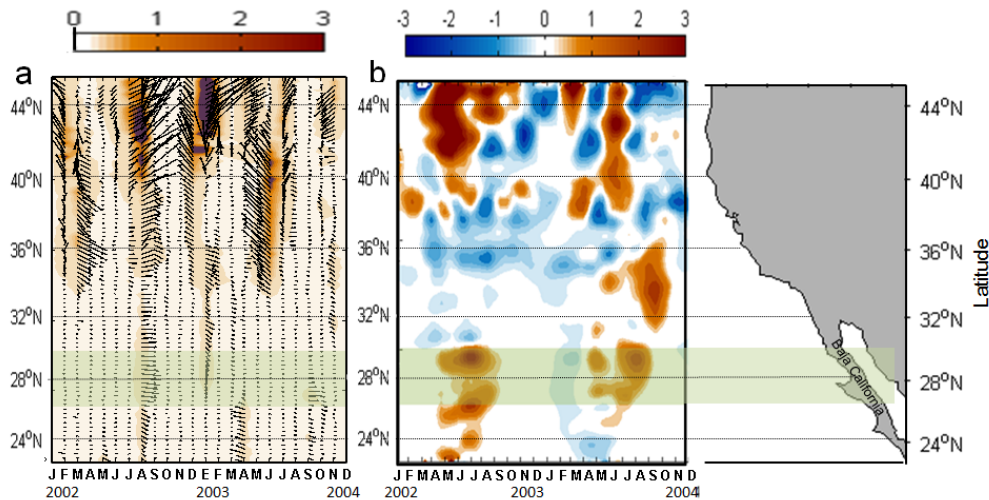


**Fig. 7.** Hovmöller diagrams of interannual anomalies of (a) monthly wind stress (magnitude and direction;  $\text{N m}^{-2} \times 10^{-2}$ ) and (b) weekly chlorophyll *a* ( $\text{mg m}^{-3}$ ) from January 2002 to December 2003 along the northeastern Pacific coast from 22 to 45° N (values within 50 km of the coast), including Punta Eugenia area (shaded in green). The wind data are provided by the CCMP project website at <http://podaac-opendap.jpl.nasa.gov/opendap/allData/ccmp/L3.0/flk/>, and weekly chlorophyll *a* by the SeaWiFS project of NASA Goddard Space Flight Center website at <http://oceancolor.gsfc.nasa.gov/>.

events are registered in SST and Chl *a*; these observations are consistent with the overall increasing (decreasing) trend of Chl *a* in the coastal (deep) zone of Punta Eugenia as indicative of weaker El Niño events (Kahru et al., 2012).

In contrast, the spatial patterns of joint EOF<sub>1</sub> showed that the SST–Chl *a* interannual covariation off Punta Eugenia is the ENSO mode. The spatial pattern of SST (Fig. 4a) showed an intense variability within the near-shore band, while the spatial pattern for Chl *a* (Fig. 4b) differs little by having high loadings more evenly centered north of Punta Eugenia, including Bahía Vizcaíno. The spatial pattern of joint SST mode coincides to the correlation map between SST and Chl *a* (Fig. 4c), having a spatial correlation of  $|R| = 0.89$ . During El Niño events, coastal-trapped waves (Durazo and Baumgartner, 2002; Dever and Winant, 2002; Jacobs et al., 1994) reach the Baja California Peninsula coast accompanied by meandering poleward flow, positive SST anomalies increase the sea surface height that deepens the nutricline and reduces the availability of nutrients to the euphotic zone. While the signals associated with La Niña events are accompanied by positive anomalies of Chl *a* associated with an intensification of the northern winds, from which the upwelling events raise the nutricline and thus increase the availability of nutrients in the coastal region of Baja California (Espinosa-Carreón et al., 2012; Chavez et al., 1999; Wooster and Hollowed, 1995). The correlation pattern, suggests that the different physical–biological responses to events such as the 1997–1999 ENSO oscillations arise from a combination of ecological and physical dynamics (Wilson and Adamec, 2001), suggesting a high biophysical coupling off Punta Eugenia during ENSO cycles (Espinosa et al., 2004). Beyond the obvious considerations, any signal of ENSO on SST and

Chl *a* would be masked by local processes (oceanic and atmospheric forcing, dissipative phenomena, upwelling) thus obscuring their statistical relationships. Therefore we believed that the similarity of the trends between the series shown in Fig. 3c and the spatial patterns shown in Fig. 4 indicate an important role of ENSO in forcing interannual variations off Punta Eugenia.

In a similar fashion, we overlaid the mean homogeneous correlation calculated for the periods El Niño–La Niña and the intrusion of subarctic water on the spatial correlation pattern (Fig. 5a) and the chlorophyll mode of the individual EOF<sub>1</sub> analysis (Fig. 5b). The region dominated for the El Niño–La Niña cycle coincide with those of the spatial distribution of intense co-variability and the high correlations between SST and Chl *a* (Fig. 4c) coincident with the region where intense coastal wind-driven upwelling and complex mesoscale variability are found (Espinosa-Carreón et al., 2012; Gonzalez-Rodríguez et al., 2012; Soto-Mardones et al., 2004) and where the propagation of coastal waves has been observed during the El Niño event (Parés-Sierra and O’Brien, 1989; Durazo and Baumgartner, 2002). The mean homogeneous correlation, calculated during the intrusion of subarctic water (solid contours in Fig. 5b), coincides significantly to that of individual EOF<sub>1</sub> (Fig. 3a, b) when analyzed over the entire time series. Although the integral timescale and the small number of effective number of degrees of freedom of these homogeneous correlations (see Table 2) leads to expected artificial correlations and cannot be regarded as significant (Davis, 1976; Chelton and Davis, 1982; and Tremberth, 1983), the spatial patterns showed that the spatial trends vary during these different remote forcing conditions (Wilson and Adamec, 2001).

Time plots of SST and Chl *a* coastal anomalies (Fig. 6b, c) showed that, MEI and CUI anomalies are not related with the intrusion of subarctic water. Espinosa-Carreón et al. (2004) suggested that on an interannual timescale, changes in the monthly CUI anomalies do not appear to be the primary source of variability in the oceanic parameters such as SST and Chl *a*, since removing the seasonal component results in low correlation values (see Table 1). The chlorophyll bloom showed during the 2002–2003 period was stronger than during the strong 1999–2000 La Niña event, evidencing that the distribution of biological groups in areas as far south as 28° N were influenced mostly by the intrusion of water of northern origin, than by events of both local and equatorial origin (positive CUI anomalies and ENSO event). These conditions, driven by the southern part of the California Current (Bograd and Lynn, 2003; Durazo et al., 2005), caused a reversal in environmental conditions opposite to the Pacific Ocean's variability shown by the MEI in this period. Durazo et al. (2005) observed at the surface the presence of zooplankton groups (salps) associated with an intrusion of subarctic water but also at depths of 100 m zooplankton groups (chaetognaths) associated with water of tropical origin that accompanies El Niño events. These observations are consistent with the overall increasing trend of Chl *a* in the upwelling coastal zone off Punta Eugenia showed by Kahru et al. (2012), either due to increased upwelling or increased nitrate concentration in the upwelled water.

The evolution of exceptionally high Chl *a* concentration along the western coast of North America during the period of subarctic water intrusion (2002–2003), can be observed in Fig. 7. This was extended toward the Equator more than 3000 km (from 45 to 22° N), a coastal area where the extension of the continental shelf, the geometry of the coastline and the local processes (wind-driven coastal upwelling and advection) play an important role in modulating the productivity. Wind stress anomalies developed north of 35° N and strengthened during spring and summer 2002, coinciding with positive Chl *a* anomalies observed along the North America coast. This could be associated with onshore large-scale advection induced by winds in the central Pacific (Chelton and Davis, 1982) or anomalous Ekman transport that may drive enhanced coastal upwelling and/or more vigorous along-coast currents (Taylor et al., 2008). It is worth noting that positive Chl *a* anomalies observed off Punta Eugenia during spring and summer 2002, could be compared to those observed north of 42° N, both could be result of the strong west wind stress anomalies and enhanced coastal upwelling developed in spring–summer 2002, increasing levels of pigment concentration above the average for the coastal zone. This bloom of positive Chl *a* anomalies occurs again during summer 2003 and is coincident with the peaks of amplitude time series of the Chl *a* individual EOF<sub>1</sub> scores (Fig. 3c).

Our study is consistent with the notion that changes in Chl *a* concentration could be due to other factors such as

decadal variability and, thus, changes in grazing pressures on the phytoplankton (Lavaniegos and Jiménez-Pérez, 2006; Wilson and Adamec, 2001) that may cause an impact on biological communities located along the coast. Gaxiola-Castro et al. (2008), using data obtained during IMECOCAL cruises (2001–2007), observed that the intrusion of subarctic water represented by an anomalous low salinity condition in the southern sector of the California Current appears to be coupled with the 2002–2006 warm phase of the Pacific Decadal Oscillation index (PDO). Neither the local upwelling (represented by the CUI anomalies) nor the zonal Ekman drift velocity used as a proxy for coastal upwelling showed signals associated with the presence of the intrusion of subarctic water. In this case, the positive signals of wind stress developed along the coast were in agreement with the bloom of the Chl *a*, mainly north of 35° N (Fig. 7).

## 5 Conclusions

Unlike the data gathered during oceanographic cruises, the temporal and spatial resolution of satellite-derived SST and Chl *a* data allowed for observation (both separately and jointly on the two fields) of the physical–biological coupling of very near-shore environments during large-scale processes that affected the region off Punta Eugenia. This region of intense biological productivity and oceanographic transition is highly influenced by the intrusion of subarctic water and by subtropical signatures triggered by poleward flow (e.g., ENSO cycles). The spatial patterns of individual EOF<sub>1</sub> could be forced mainly by an unusual enhanced onshore transport of subarctic water observed mainly during the period 2002–2004, defined by Goericke et al. (2005) as a cold phase of the CCS. Whereas the physical–biological coupling was forcing mainly by interannual variability of local and equatorial origin (CUI and ENSO events) tightly observed in an alongshore band of ~40 km wide. The Hovmöller diagram of coastal SST and Chl *a* anomalies calculated from September 1997 to December 2007 and the homogeneous correlation calculated during the strong 1997–1999 El Niño–La Niña time period, delineated the regions that contribute the most to the ENSO mode.

Although, some ENSO events dominated the area for a long time, the presence of the intrusion of subarctic water off Punta Eugenia might have had a greater influence on the individual interannual variability of both SST and Chl *a* variables. This remote forcing results in a large-scale chlorophyll bloom that extends for more than 3000 km of the northeastern Pacific coast (22–45° N) showing that Punta Eugenia is one of the most important biological action centers of the western coast of North America with levels of pigment concentration comparable to those found at higher latitudes (Oregon coast). These results successfully support the data from previous hydrographic surveys (CaLCOFI and IMECOCAL programs) off Baja California.

**Supplementary material related to this article is available online at <http://www.ocean-sci.net/10/345/2014/os-10-345-2014-supplement.pdf>.**

*Acknowledgements.* Ira Fogel of CIBNOR provided editorial improvements. We thank E. Beier (CICESE-BCS) for helpful comments. We thank the Pathfinder and SeaWiFS projects and the NASA Physical Oceanography Distributed Active Archive Center for the production and distribution of AVHRR-SST and SeaWiFS data. This research was funded by SAGARPA CONACYT grants 2009-113C. Additional thanks go to the anonymous reviewers who gave valuable comments on an earlier draft of the manuscript.

Edited by: M. Kosro

## References

- Almazán-Becerril, A., Rivas, D., and García-Mendoza, E.: The influence of mesoscale physical structures in the phytoplankton taxonomic composition of the subsurface chlorophyll maximum off Baja California, *Deep-Sea Res.-Pt. I*, 70, 91–102, 2012.
- Behrenfeld, M. J., O'Malley, R. T., Siegel, D. A., McClain, C. R., Sarmiento, J. L., Feldman, G. C., Milligan, A. J., Falkowski, P. G., Letelier, R. M., and Boss, E. S.: Climatic-driven trends in contemporary ocean productivity, *Nature*, 444, 752–755, 2006.
- Bretherton, C. S., Smith, C., and Wallace, J. M.: An intercomparison of methods for finding coupled patterns in climate data, *J. Climate*, 5, 541–560, 1992.
- Boehm, A. B., Lluch-Cota, D. B., Davis, K. A., Winnan C. D., and Monismith, S. G.: Covariation of coastal water temperature and microbial pollution at interannual to tidal periods, *Geophys. Res. Lett.*, 31, L06309, doi:10.1029/2003GL019122, 2004.
- Bograd, S. J. and Lynn, R. J.: Anomalous subarctic influence in the southern California Current during 2002, *Geophys. Res. Lett.*, 30, 8020, doi:10.1029/2003GL017446, 2003.
- Carreón-Palau, L., Guzman Del, P. S. A., Belmar, J. P., Carrillo, J. L., and Herrera, R. F.: Microhábitat y biota asociada a juveniles de abulón *Haliotis fulgens* y *Haliotis corrugata* en bahía Tortugas, Baja California Sur, México, *Ciencias Marinas*, 29, 325–341, 2003.
- Chavez, F. P., Strutton, P. G., Friederich, G. E., Feely, R. A., Feldman, G. C., Foley, D. G., and McPhaden, M. J.: Biological and chemical response of the equatorial Pacific to the 1997–1998 El Niño, *Science*, 286, 2126–2131, 1999.
- Chelton, D. B.: Statistical reliability and the seasonal cycle: comments on “Bottom pressure measurements across the Antarctic Circumpolar Current and their relation to the wind”, *Deep-Sea Res.*, 29, 1381–1388, 1982.
- Chelton, D. B. and Davis, R. E.: Monthly mean sea level variability along the west coast of North America, *J. Phys. Oceanogr.*, 12, 757–784, 1982.
- Davis, R. E.: Predictability of sea surface temperature and sea level pressure anomalies over the North Pacific Ocean, *J. Phys. Oceanogr.*, 6, 249–266, 1976.
- Dever, E. P. and Winant, C. D.: The evolution and depth structure of shelf and slope temperatures and velocities during the 1997–1998 El Niño near Point Conception, California, *Prog. Oceanogr.*, 54, 77–103, 2002.
- Durazo, R. and Baumgartner, T. R.: Evolution of oceanographic condition off Baja California: 1997–1998, *Prog. Oceanogr.*, 54, 7–31, 2002.
- Durazo, R., Gaxiola-Castro, G., Lavaniegos, B., Castro-Valdez, R., Gómez-Valdez, J., and Mascarenhas Jr., A. S.: Oceanographic conditions off the western Baja California coast, 2002–2003: A weak El Niño and subarctic water enhancement, *Ciencias Marinas*, 31, 537–552, 2005.
- Espinosa-Carreón, L., Strub, P. T., Beier, E., Ocampo-Torres, F., and Gaxiola-Castro, G.: Seasonal and interannual variability of satellite-derived chlorophyll pigment surface height, and temperature off Baja California, *J. Geophys. Res.*, 109, C03039, doi:10.1029/2003JC002105, 2004.
- Espinosa-Carreón, L., Gaxiola-Castro, G., Beier, E., Strub, P. T., and Kurczyn, J. A.: Effect of mesoscale processes on phytoplankton chlorophyll off Baja California, *J. Geophys. Res.*, 117, C04005, doi:10.1029/2011JC007604, 2012.
- Freeland, H. J., Gatién, G., Huyer, A., and Smith, R. L.: A cold halocline in the northern California current: an invasion of subarctic water, *Geophys. Res. Lett.*, 30, 1141, doi:10.1029/2002GL016663, 2003.
- Gallaudet, T. C. and Simpson, J. J.: An empirical orthogonal function analysis of remotely sensed sea surface temperature variability and its relations to interior oceanic processes off Baja California, *Remote Sens. Environ.*, 47, 374–389, 1994.
- Gaxiola-Castro, G., Durazo, R., Lavaniegos, B., De-la-Cruz-Orozco, M. E., Millán-Núñez, E., Soto-Mardones, L., and Cepeda-Morales, J.: Pelagic ecosystem response to interannual variability off Baja California, *Ciencias Marinas*, 34, 263–270, 2008.
- Goericke, R., Venrick, E., Mantyla, A., Bograd, S. J., Schwing, F. B., Huyer, A., Smith, R. L., Wheeler, P. A., Hoff, R., Peterson, W. T., Chavez, F., Collins, C., Marinovic, B., Lo, N., Gaxiola-Castro, G., Durazo, R., Hyrenbach, K. D., and Sydeman, W. J.: The state of the California Current, 2004–2005: Still cool?, *CalCOFI Rep.*, 46, 32–71, 2005.
- González-Rodríguez, E., Trasviña-Castro, A., Gaxiola-Castro, G., Zamudio, L., and Cervantes-Duarte, R.: Net primary productivity, upwelling and coastal currents in the Gulf of Ulloa, Baja California, México: *Ocean Science*, 8, 703–711, 2012.
- Hereu, C. M., Jiménez-Pérez, L. C., and Lavaniegos, B. E.: Effects of the El Niño 1997–1998 and the rapid transition to cool conditions in the winter 1998–1999 on the copepods and salps of the California Current. 3rd International Zooplankton Production Symp., 20–23 May 2003, Gijón Spain, Program and Abstracts, p. 53, 2003.
- Huyer, A.: Preface to special section on enhanced subarctic influence in the California Current, 2002, *Geophys. Res. Lett.*, 30, 8019, doi:10.1029/2003GL017724, 2003.
- Jacobs, G. A., Hulburt, H. E., Kindle, J. C., Metzger, E. J., Mitchell, J. L., Teague, W. J., and Wallcraft, A. J.: Decade-scale trans-Pacific propagation and warming effect of an El Niño anomaly, *Nature*, 370, 360–363, 1994.
- Kahru, M. and Mitchell, B. G.: Influence of the 1997–98 El Niño on the surface chlorophyll in the California Current, *Geophys. Res. Lett.*, 27, 2937–2940, 2000.

- Kahru, M. and Mitchell, B. G.: Seasonal and nonseasonal variability of satellite-derived chlorophyll and colored dissolved organic matter concentration in the California Current, *J. Geophys. Res.*, 106, 2517–2529, 2001.
- Kahru, M., Kudela, R. M., Manzano-Sarabia, M., and Mitchell, B. G.: Trends in the surface Chlorophyll of the California Current: Merging data from multiple ocean color satellites, *Deep-Sea Res.-Pt. II*, 77–80, 89–98, 2012.
- Kosro, P. M.: Enhanced southward flow over the Oregon shelf in 2002: A conduit for subarctic water, *Geophys. Res. Lett.*, 30, 8023, doi:10.1029/2003GL017436, 2003.
- Lavaniegos, B. E. and Jiménez-Pérez, L. C.: Biogeographic inferences of shifting copepod distribution during 1997–1999 El Niño and La Niña in the California Current, *Contributions to the Study of East Pacific Crustaceans*, 4, 113–158, 2006.
- Lavaniegos, B. E., Jiménez-Pérez, L. C., and Gaxiola-Castro, G.: Plankton response to El Niño 1997–1998 and La Niña 1999 in the southern region of the California Current, *Prog. Oceanogr.*, 54, 33–58, 2002.
- Lluch-Belda, D., Elorduy-Garay, J., Lluch-Cota, S. E., and Ponce-Díaz, G.: BAC Centros de Actividad Biológica del Pacífico Mexicano. Centro de Investigaciones Biológicas del Noroeste, Centro Interdisciplinario de Ciencias Marinas, Consejo Nacional de Ciencia y Tecnología, La Paz, B.C.S., Mexico, 2000.
- Mitchell, B. G.: Bio-optical measurements and modeling of the California Current and Southern Oceans, Final Report, Scripps Institution of Oceanography, University of California San Diego, La Jolla, CA 92093-0218, 27 pp., 2004.
- Muciño-Días, M., Sierra-Rodríguez, O. P., Castro, J. J., Talavera, J. J., Turrubiates, J. R., Caballero, F., and Rivera, J. L.: Estado de las poblaciones de Abulon azul *Haliotis fulgens* y amarillo *H. corrugata* por zona reglamentada en la costa occidental de la península de Baja California, Temporada 2003/2004, Dictamen Técnico, Instituto Nacional de la Pesca. Dirección general de Investigación pesquera en el Pacífico Norte, 12 pp., 2004.
- O'Really, J. E., Maritorena, S., O'Brien, M. C., Siegel, D. A., Toole, D., Menzies, D., Smith, R. C., Mueller, J. L., Mitchell, B. G., Kahru, M., Chavez, F. P., Strutton, P., Cota, G. F., Hooker, S. B., McClain, C. R., Carder, K. L., Müller-Karger, F., Harding, L., Magnuson, A., Phinney, D., Moore, G. F., Aiken, J., Arrigo, K. R., Letelier, R., and Culver, M.: SeaWiFS Postlaunch Calibration and Validation Analyses, Part 3, edited by: Hooker, S. B. and Firestone, E. R., NASA Tech. Memo. 2000-206892. NASA Goddard Space Flight Center, Vol. 11, 49 pp., 2000.
- Palacios, H. E., Argote, M. L., Amador A., and Mancilla, M.: Simulación de la circulación barotrópica inducida por viento en Bahía Sebastián Vizcaíno, B.C., *Atmósfera*, 9, 171–188, 1996.
- Parés-Sierra, A. and O'Brien, J. J.: The seasonal and interannual variability of the California Current System: A numerical model, *J. Geophys. Res.*, 93, 3159–3180, 1989.
- Parés-Sierra, A., Lopez, M., and Pavía, E.: Oceanografía Física del Océano Pacífico Nororiental, in *Contribuciones a la Oceanografía Física en México*, Monograf. Ser. Vol. 3, Unión Geofísica Mexicana, Puerto Vallarta, México, 1–24, 1997.
- SAGARPA: Anuario estadístico de pesca, 2001, Comisión Nacional de Pesca y Acuicultura, México, 2001.
- SAGARPA: Anuario estadístico de pesca, 2011, Comisión Nacional de Pesca y Acuicultura, México, 2011.
- SEMARNAT: Secretaría de Medio Ambiente Recursos Naturales: Salitrales de San Ignacio, sal y ballenas en Baja California, México, 1997.
- Sciremammano, F.: A suggestion for the presentation of correlation and their significance level, *J. Phys. Oceanogr.*, 9, 1273–1276, 1979.
- Schwing, F. B. and Mendelssohn, R.: Increased coastal upwelling in the California Current System, *J. Geophys. Res.*, 102, 3421–3438, doi:10.1029/96JC03591, 1996.
- Soto-Mardones, L., Parés-Sierra, A., García, J., Durazo, R., and Hormazabal, S.: Analysis of the mesoscale structure in the IME-COCAL region (off Baja California) from hydrographic, ADCP and altimetry data, *Deep-Sea Res.-Pt. II*, 51, 785–798, 2004.
- Storch, H. V. and Zwiers, F. W. (Eds.): *Statistical analysis in climate research*. Cambridge University Press, Cambridge, 1999.
- Strub, P. T. and James, C.: Altimeter-derived surface circulation in the large-scale Pacific gyres. Part 2: 1997–1998 El Niño anomalies, *Prog. Oceanogr.*, 53, 185–214, 2002.
- Taylor, S. V., Cayan, D. R., Graham, N. E., and Georgakakos, K. P.: Northerly surface winds over the eastern North Pacific ocean spring and summer, *J. Geophys. Res.*, 113 D02110, doi:10.1029/2006JD008053, 2008.
- Trenberth, K. E.: Signal Versus Noise in the Southern Oscillation, *Mon. Weather Rev.*, 112, 326–332, 1983.
- Vega, A. V.: Reproductive strategies of the spiny lobster *Panulirus interruptus* related to the marine environmental variability off central Baja California, México: management implications, *Fish. Res.*, 65, 123–135, 2003.
- Vega, A., Treviño, E., Gracia, G., Espinoza-Castro, L., and Zuñiga-Pacheco, C.: Evaluación de la langosta roja (*Panulirus interruptus*) en la región centro occidental de la península de Baja California, mediante modelos dinámicos de biomasa: puntos de referencia y recomendaciones de manejo. Informe de Investigación, Instituto nacional de la Pesca, 21 pp., 2010.
- Venrick, E., Bograd, S., Checkley, D., Cummings, S., Durazo, R., Gaxiola-Castro, G., Hunter, J., Huyer, A., Hyrenbach, K., Lavaniegos, B., Mantyla, E. A., Schwing, F. B., Smith, R. L., Syderman, W. J., and Wheeler, P. A.: The state of the California Current, 2002–2003: Tropical and subarctic influences vie for dominance, *CalCOFI Report*, 44, 28–60, 2003.
- Wilson, C. and Adamec, D.: Correlation between chlorophyll and sea surface height in the tropical Pacific during 1997–1999 El Niño Southern Oscillation event, *J. Geophys. Res.*, 106, 31175–31188, 2001.
- Wolter, K. and Timlin, M. S.: Monitoring ENSO in COADS with a seasonally adjusted principal component index. Proc. 17th Climate Dynamics Workshop; Norman, OK, NOAA/NMC/CAC, NSSL, Oklahoma Clim. Survey, CIMMS and School of Meteorology, Univ. Oklahoma, Norman, OK, 52–57, 1993.
- Wooster, W. S. and Hollowed, A. B.: Decadal scale variations in the eastern subarctic Pacific. I. Winter ocean conditions, Climate change and northern fish populations, edited by: Beamish, R. J., *Canadian Spec. Publ. Fish. Aquatic Sci.*, 121, 81–85, 1995.